

Research Article

Microstructure, Mechanical, and Magnetic Properties of Medium Manganese Steel Subjected to ART Heat Treatment Cycle

J. N. Mohapatra^{1*}, M. Vidhyasagar², D. Satish Kumar¹

¹JSW Steel Ltd., Vijaynagar Works, Toranagallu, 583275, Bellary Karnataka, India

²JSW Steel Ltd., Salem Works, Tamilnadu, 636453, India

E-mail: jitendra.mohapatra@jsw.in

Received: 23 April 2025; Revised: 7 July 2025; Accepted: 16 July 2025

Abstract: A type of low-carbon (0.19 wt.% C), medium-manganese (6.67% Mn) steel containing 0.78% Al was cast and converted into 2 mm thick wrought steel. This type of steel was subjected to austenitization at a temperature range of 600 to 800 °C with 20 °C steps, followed by air cooling, to develop the third-generation Advanced High-Strength Steel (AHSS). Microstructural changes were analyzed through Electron Backscattered Diffraction (EBSD), mechanical properties were assessed through tensile testing, and magnetic properties were evaluated and correlated to enable potential Non-Destructive Evaluation (NDE) of the heat treatment conditions and property variations. With an increase in austenitization temperature, the strengths (Yield Strength (YS) and Ultimate Tensile Strength (UTS)) were decreased, while total elongation in the steel increased up to around 680-700 °C, and then a reversing trend was found. The strength-elongation product was found to be maximum (> 30 GPa.%) at such a temperature range due to the Transformation Induced Plasticity (TRIP) effect from the presence of the maximum amount of Retained Austenite (RA) in addition to bainitic phases. A decrease in remanence and maximum induction was found with the increase in coercivity as RA content increased in the steel up to 700 °C, and then a reversing trend was found, with the exception of coercivity, which peaked at 720 °C. Hence, by measuring the maximum induction in the steel, the retained austenite content can be estimated, which is responsible for the TRIP effect in the steel.

Keywords: medium manganese steel, Austenite Reverted Transformation (ART) heat treatment, microstructure, mechanical properties, magnetic properties

1. Introduction

Steels with a manganese content of 3-12% Mn are experiencing growing demand in the automotive industry for the development of third generation Advanced High Strength Steels (AHSS) [1]-[5]. The excellent properties develop due to the transformation of metastable austenite to martensite while deformation, known as the TRIP effect. A detailed review on the medium manganese steels regarding their microstructure and mechanical properties has been reported in the literature [6]-[8]. The steels after forging and air cooling exhibit lower volume fraction of Retained Austenite (RA) while Inter Critical Annealing (ICA) at low temperature leads to further decrease in the matrix strength due to carbides dissolution. ICA at intermediate annealing temperature facilitates carbon partitioning and the formation of globular austenite islands at the prior austenite grain boundaries within the martensitic matrix, resulting in increased

Copyright ©2025 J. N. Mohapatra, et al.
DOI: <https://doi.org/10.37256/est.6220257075>
This is an open-access article distributed under a CC BY license
(Creative Commons Attribution 4.0 International License)
<https://creativecommons.org/licenses/by/4.0/>

ductility and toughness without a change in its strength. Beyond the optimum ICA temperature, both volume fraction increase and morphology change of austenite occurs forming a coarse network [9]. Several studies depict microstructure and mechanical properties of these steels [10]-[12], whereas almost no literature found on the study of their physical properties. Measuring the physical properties will help in non-destructive evaluation of heat treatment conditions and phase changes that affect them. Structure sensitive magnetic properties of steels are gaining popularity for the evaluation of heat treatment or welding induced microstructural changes. Hence, by measuring magnetic properties, changes in the mechanical properties resulting from the microstructural modifications can be assessed. The magnetic properties on TRIP steel have been reported earlier [13]-[15]. The presence of retained austenite increase the coercivity and drastically decrease the remanence and maximum induction whereas transformation of RA to martensite further increase the coercivity due to this hard magnetic phase and its interaction with the dislocations.

In the present study, a low-carbon (0.19 wt.% C), medium-manganese (6.67% Mn) steel with 0.78% Al was forged and air-cooled, then subjected to inter-critical austenitization at temperatures ranging from 600 to 800 °C to form reverted austenite, aiming to obtain various microstructure and mechanical properties with the aim to develop third generation AHSS. The microstructure and magnetic properties were correlated with the change in mechanical properties of the steel for their NDE.

2. Experimental

The steel was melted in a 25 kg capacity air induction furnace and cast into a 10 kg ingot, which was heated to a soaking temperature 1,200 °C for 3 hours and forged to convert the cast structure to wrought steel. The cast ingot was subjected to 85% reduction to a final size of 65 × 65 mm² billet. The billets were sliced to 2 mm thick strips using Electric Discharge Machine (EDM) and heat-treated in a muffle furnace. The forged and air-cooled steel was subjected to Austenite Reverted Transformation (ART) through re-austenitization (reheating to temperatures ranging from 600 to 800 °C with a step of 20 °C and holding for 5 min) followed by air cooling. The ART heat treatment cycle is shown in Figure 1.

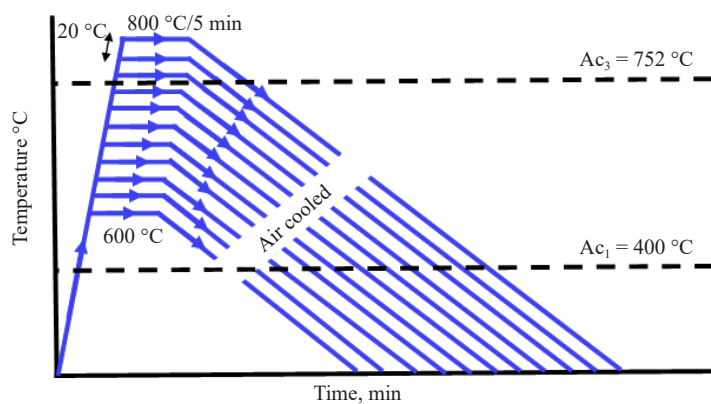


Figure 1. ART heat treatment cycle applied to the as-forged and 2 mm sliced steel

The chemical composition of the steel was determined using SPECTRO optical emission spectroscopy. Heat-treated samples were cut using an EDM machine to prepare standard ASTME8M samples for tensile test; more details on the test can be found in literature [13]. The EBSD analysis of the steel was conducted through a Hitachi Scanning Electron Microscopy (SEM) (Model: S3400N). After the sample was polished with a mirror surface, it was subjected to electrolytic polishing treatment. Finally, the phase fraction was determined under the conditions of a magnification of 4,000 X, a scanning area of 80 × 90 μm, and a step size of 0.9 μm.

Magnetic Hysteresis Loop (MHL) measurements were conducted using a portable Non-Destructive Evaluation (NDE) device-*MagStar* through a surface probe on the strip surface at specified field strength and frequency to obtain

major hysteresis loops [13], [16]. The MHL measurements were conducted from both sides of the strips and averaged for the evaluation of their standard deviations.

3. Results and discussion

Table 1 shows chemical composition of the steel. It has 0.19% C which ensures good weldability due to low carbon equivalent. With 6.67% Mn (an austenite-stabilizing element), the steel exhibits shifted Ac_1 temperature to 400 °C and Ac_3 to 752 °C, as evaluated (calculated) using thermocalc software (2020b Steel and Fe-alloys databases). The high Mn content also shifts the C-curve in the Continuous Cooling Transformation (CCT) diagram to the right, promoting martensite formation even under air cooling. The 0.78% Al content suppresses the carbide formation tendency in the steel while promoting the formation of austenite. As the steel is not having high Si content unlike other high Mn steel, the present steel can be coated as well. The other elements in the steel are residual elements that were not purposely added. The S content is 0.001% and P content is 0.013%. Residual Cu and Ni are beneficial as they are austenite stabilizers. The Cr content is also not a detrimental element for the properties, as it improves the yield strength and tensile strength without the loss of uniform elongation [17].

Table 1. Chemical composition of the steel (wt.%)

C	Mn	Si	S	P	Al	Cr	Ni	Cu	N
0.19	6.67	0.30	0.001	0.013	0.78	0.085	0.011	0.029	0.03

$Ac_1 = 400$ °C; $Ac_3 = 752$ °C (Based on ThermoCalc calculation)

3.1 EBSD

EBSD analysis of the as-forged medium manganese steel with its image quality map (a), color-coded phase map (b), and grain boundary map (c) is shown in Figure 2. The steel in as-forged condition shows 53.8% ferrite, 32.8% bainite, and 9.3% martensite, and a low (4%) retained austenite. It indicates that the RA has been transformed to bainite and martensite during air cooling after forging at high temperature. In the case of grain boundary mapping for statistics, any point pairs with mis-orientation exceeding 2° is considered a boundary.

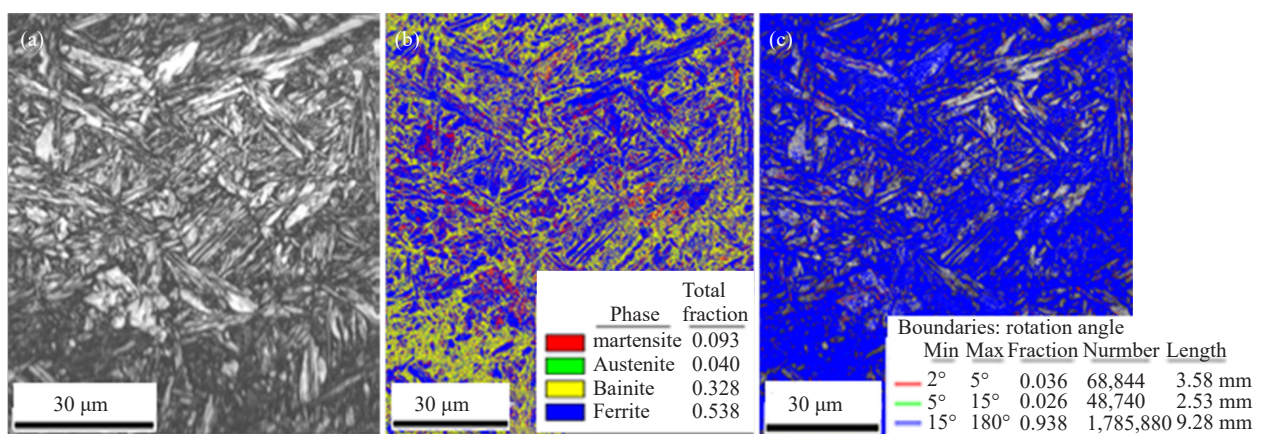


Figure 2. EBSD analysis of as-forged medium manganese steel

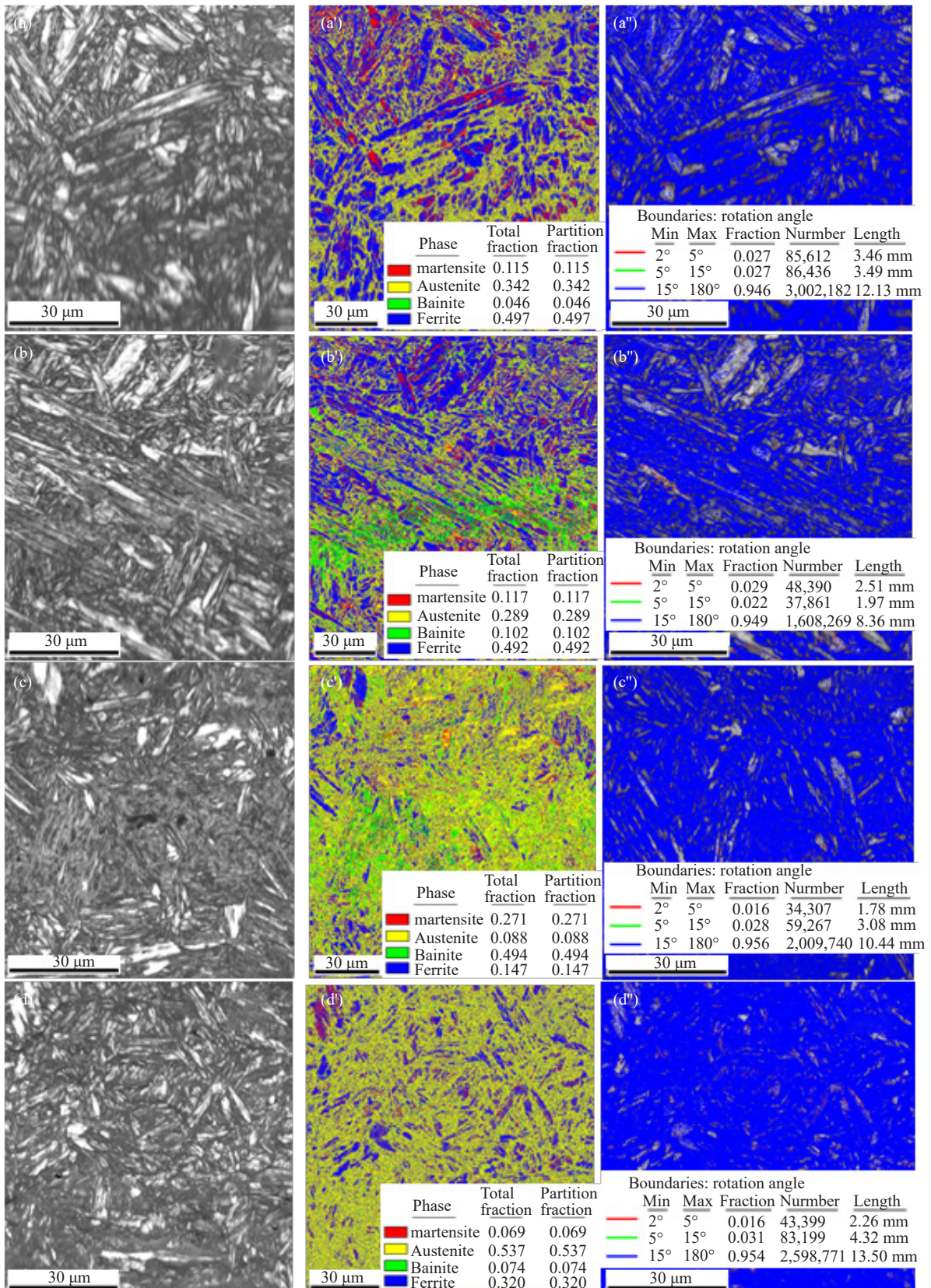


Figure 3. EBSD analysis of the medium manganese steel austenitized at (a) 600 °C, (b) 680 °C, (c) 700 °C, and (d) 800 °C, with corresponding (a')-(d') and (a'')-(d'') color-coded phase map and grain boundary map, respectively

The EBSD of the medium manganese steel austenitized at (a) 600 °C, (b) 680 °C, (c) 700 °C, and (d) 800 °C is shown in Figure 3 with (a')-(d'), and (a'')-(d'') are their corresponding color coded phase map and grain boundary map, respectively. The phase fractions found at different conditions are summarized in Table 2. The observation shows that the RA volume fraction has been increased and in the range of 10-15% at the temperature range of 680-700 °C and then decreased with further increase in austenitization temperature. In addition to the RA, martensite volume fractions were also increased and then decreased after a peak at 680 °C. The bainite content in the steel increased with the reduction in ferrites with the rise in austenitization temperature. Hence, at the peak temperature range of 680-700 °C, ferrite between 27-49%, bainite between 29-49%, martensite between 9-12%, and RA between 10-15% formed. The higher content of RA is due to the austenite reverted transformation in the narrow temperature range. Higher RA content will lead to transformation to martensite during deformation by TRIP effect, thereby achieving a better combination of mechanical properties and higher energy absorption in crash condition, which provides safety protection for passengers. Hence, this type of steel is preferred in automotive safety components [18]. Furthermore, dislocation-phase transformation interactions during austenite-to-martensite conversion contribute to strength improvement.

Table 2. Phase fraction obtained through EBSD analysis

Condition	Ferrite (α)	Bainite (α_B)	Martensite (α')	Retained austenite (γ)
As-Forged	53.8	32.8	9.3	4
600 °C/5 min/AC	49.7	34.2	11.5	4.6
680 °C/5 min/AC	49.2	28.9	11.7	10.2
700 °C/5 min/AC	27.1	49.4	8.8	14.7
800 °C/5 min/AC	32	53.7	6.9	7.4

3.2 Mechanical properties

The changes in Yield Strength (YS), Ultimate Tensile Strength (UTS), and Total Elongations (TE) of the as-forged and ART heat-treated steels are shown in Figure 4. The YS and UTS of the steel showed a decreasing trend up to around 700 °C and then increased with a reverse trend for TE.

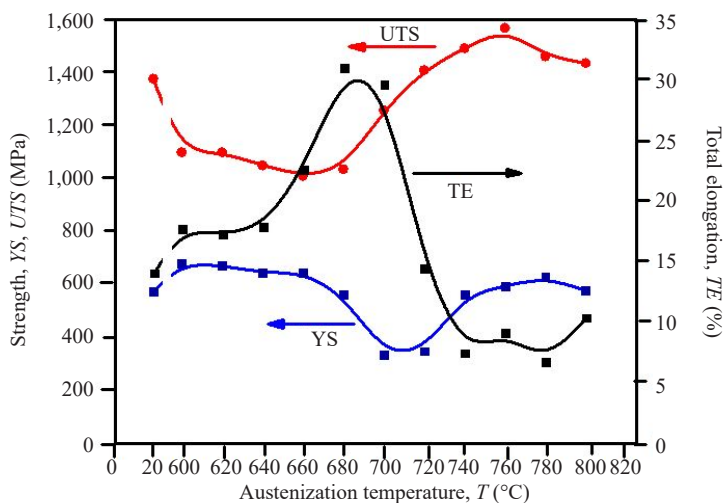


Figure 4. Changes in YS, UTS, and TE of as-forged steel with increase in annealing temperature

As mentioned in the EBSD analysis section, the steel in as-forged condition shows 53.8% ferrite, 32.8% bainite,

9.3% martensite and a low (4%) RA. The complex phases in the steel gave high YS (573 MPa), high UTS (1,377 MPa), and TE of 14.07%. A high level of dislocations and residual stress is expected in the as-forged condition. With annealing at 600 °C, the dislocations gets annihilated and the residual stress in the steel decreased, resulting in a drop in strength. With increase in annealing temperature, a very small decrease in YS and UTS occurred with a rise in the ductility of the steel. As the temperature rises, the volume fraction of ferrite decreases with an increase in bainite, martensite, and RA, making the TRIP effect more prominent and resulting in increased ductility in the steel at 700 °C. With further increase in temperature, the volume fraction of RA decreases, leading to a decrease in TE. However, the rise in strength is due to further enhancement of bainite volume fraction with decreasing ferrite content in the steel.

3.3 Magnetic properties

The MHL of the medium manganese steel in the as-forged and air-cooled condition and subjected to ART at temperatures from 600 to 700 °C (with 20 °C step, holding time of 5 min, and air-cooled condition) is shown in Figure 5a. The samples subjected to ART heat treatment between 700 °C and 800 °C with 20 °C step are shown in Figure 5b.

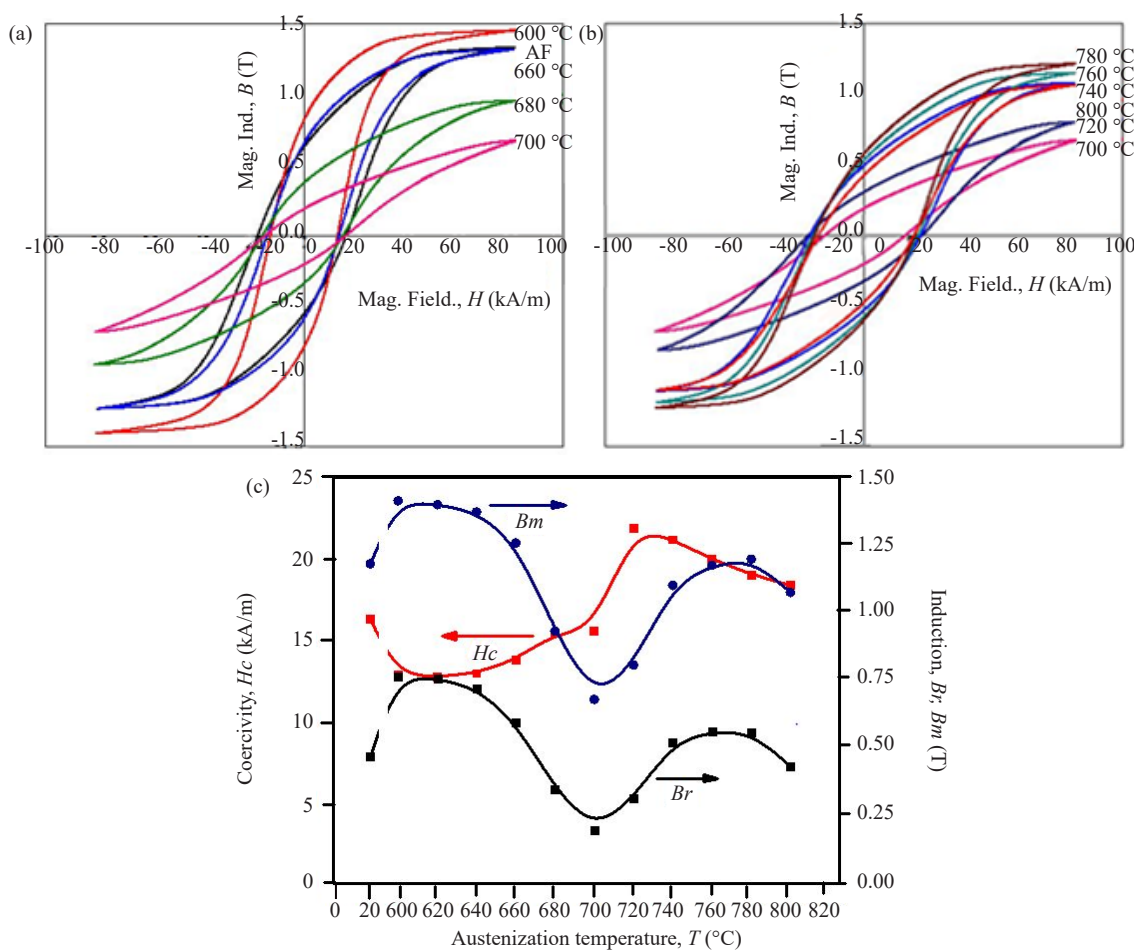


Figure 5. Magnetic hysteresis loop of the As-Forged (AF) and annealed medium manganese steel: (a) 600-700 °C for 5 min followed by air cooling, (b) 700-800 °C, and (c) changes in coercivity, remanence and maximum induction

The structure-sensitive magnetic properties, such as coercivity (H_c), remanence (B_r), and maximum induction (B_m), are shown in Figure 5c. It is observed that the B_r and B_m are decreasing with rising re-austenization temperature, reaching a minima at 700 °C before recovery. The MHL width increases with rising annealing temperature, peaking at 720 °C, followed by a decreasing trend of the H_c . The coercivity is the magnetic hardness, that is, the negative force or

field required to reduce the residual magnetism to zero. H_c rises with obstacles for the magnetic domain wall motions, such as grain boundaries, dislocations, or strain field of dislocations, as well as precipitates and secondary phases in steels. The change in maximum induction mostly occurs due to the change of phases in the steel, such as hard magnetic martensite, the non-magnetic austenite, which is non-magnetic in nature, and the weakly magnetic cementite. The remanence can be changed by pinning and phase change in steels, in addition to residual stress variations.

Up to 700 °C, a rise in the volume fraction of RA in the steel will lead to a decrease in remanence and the maximum induction, as the non-magnetic phase in the steel increases. However, the coercivity is increased due to the more obstacle to magnetic domain wall for the non-magnetic austenites or strain field of dislocations. With the increase in annealing temperature beyond 700 °C, the remanence and magnetic inductions increase, while the coercivity decreases. This is due to the decrease in non-magnetic phase in the steel.

As RA is a non-magnetic phase, its increase in volume fraction leads to the decrease in the remanence and the maximum induction. However, during the transformation of RA to martensite, although martensite is a hard magnetic phase, the remanence and maximum induction increase as the hard magnetic phase increases at the expense of the non-magnetic phase. The coercivity of the steel increases due to the domain wall pinning by the non-magnetic RA phases.

3.4 Fractography

The fractography of the tensile tested steel in as-forged and air-cooled conditions and after re-austenitization at three temperatures of 600 °C, 700 °C, and 800 °C is shown in Figure 6a-d. The as-forged, air-cooled steel shows a fine dimple structure. The tempered martensite/bainite microstructure in this condition, with low retained austenite, fails by pure ductile mode, with fine dimples indicative of good ductility and toughness in the steel.

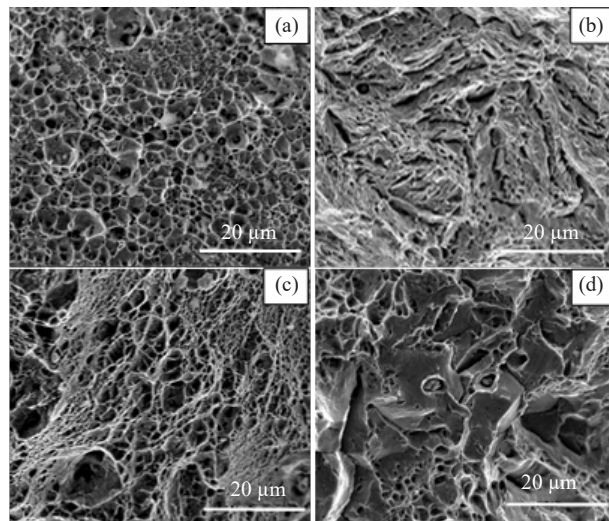


Figure 6. Fractography of the steel after tensile testing on (a) as-forged, (b) 600 °C/5 min/AC, (c) 700 °C/5 min/AC, and (d) 800 °C/5 min/AC

The fractography of the steel at 600 °C re-austenitization shows complete dimple rupture but with cracks running perpendicular to the plane of the fracture. The filmy retained austenite lies along the tempered martensite laths, and differential deformation among the phases can be observed. The steel re-austenitized at 700 °C showed a fully dimple rupture associated with tempered martensite/bainite and the highest amount of retained austenite fraction. There are small dimples due to tempered martensite, and the larger dimples may be associated with retained austenite. The fractography of the steel at 800 °C re-austenitization condition showed deep dimples but there are quasi cleavage features, indicating a mix mode of fracture.

4. Conclusions

The microstructure, mechanical properties, and magnetic properties of a medium manganese steel with 0.17% C, 6.67% Mn, and 0.78% Al subjected to Austenite Reverted Transformation (ART) heat treatment were evaluated in the present study. The following conclusions were made:

- The strengths (YS, UTS) of the steel decreased with an increase in ductility (TE) with a rise in ART temperature up to 700 °C due to the enhancement of bainite, martensite, and retained austenite, with the dominance of TRIP effect.
- With further increase in ART temperature, the properties were reversed due to the reduction in volume fraction of retained austenite, the increase in bainite content, and the decrease in ferrite content within the steel.
- Third-generation AHSS properties were obtained in a narrow temperature range of 680-700 °C, with the product of UTS and total elongation > 30 GPa.% due to the dominance of TRIP effect from the presence of a higher amount of retained austenite.
- The coercivity increased with ART temperature due to the strong pinning of the RA, resulting in a drop in maximum induction and remanence up to 700 °C, after which the properties were reversed due to the decrease in retain austenite and increase in bainite in the steel.

Conflict of interest

The authors declare that they have no known competing financial interests or personal relationships that could have appeared to influence the work reported in this paper.

References

- [1] D. W. Suh and S. J. Kim, "Medium Mn transformation-induced plasticity steels: Recent progress and challenges," *Scripta Materialia*, vol. 126, pp. 63-67, 2017.
- [2] D. P. Yang, D. Wu, and H. L. Yi, "Reverse transformation from martensite into austenite in a medium-Mn steel," *Scripta Materialia*, vol. 161, pp. 1-5, 2019.
- [3] A. Gramlich and W. Bleck, "Tempering and intercritical annealing of air-hardening 4 wt% medium manganese steels," *Steel Research International*, vol. 92, no. 1, pp. 2100180, 2021.
- [4] A. K. Verma and A. Kumar, "Microstructure and mechanical properties of medium manganese steels," *Materials Today: Proceedings*, vol. 56, no. 1, pp. 356-367, 2022.
- [5] B. Hu, X. Shen, Q. Y. Guo, Q. H. Wen, X. Tu, C. C. Ding, F. L. Ding, W. W. Song, and H. W. Luo, "Yielding behavior of triplex medium Mn steel alternated with cooling strategies altering martensite/ferrite interfacial feature," *Journal of Materials Science & Technology*, vol. 126, pp. 60-70, 2022.
- [6] S. Yan, T. L. Li, T. S. Liang, and X. H. Liu, "Adjusting the microstructure evolution, mechanical properties and deformation behaviors of Fe-5.95Mn-1.55Si-1.03Al-0.055C medium Mn steel by cold-rolling reduction ratio," *Journal of Materials Research and Technology*, vol. 9, no. 2, pp. 1314-1324, 2020.
- [7] T. L. Li, S. Yan, and X. H. Liu, "Microstructure and tensile behaviors for a medium Mn steel with d-ferrite phase under different annealing temperatures," *Journal of Materials Research and Technology*, vol. 15, pp. 708-718, 2021.
- [8] Y. Zhang, Q. Z. Ye, and Y. Yan, "Processing, microstructure, mechanical properties, and hydrogen embrittlement of medium-Mn steels: A review," *Journal of Materials Science & Technology*, vol. 201, pp. 44-57, 2024.
- [9] W. Bleck, T. Allam, and A. Gramlich, "Alloying and processing of medium manganese steels for forging applications," *BHM Berg-und Hüttenmännische Monatshefte*, vol. 167, no. 11, pp. 534-537, 2022.
- [10] R. Letak, L. Kucerova, H. Jirkova, S. Jenicek, and F. Votava, "Changes in mechanical properties of medium manganese steel after forming, press hardening, and heat treatment," *Materials*, vol. 18, no. 6, pp. 1196, 2025.
- [11] T. Kang, Z. Y. Zhan, C. C. Wang, Z. Z. Zhao, J. H. Liang, and L. L. Yao, "Microstructure evolution and tensile properties of medium manganese steel heat treated by two-step annealing," *Metals*, vol. 14, no. 9, pp. 1008, 2024.
- [12] A. Skowronek, Adam Grajcar, and R. H. Petrov, "Dependence of mechanical properties on the phase composition of intercritically annealed mediumMn steel as the main competitor of highstrength DP steels," *Scientific Reports*, vol. 14, pp. 9567, 2024.

- [13] J. N. Mohapatra and A. K. Akela, "Magnetic evaluation of tensile deformation behaviour of TRIP assisted steels," *Journal of Nondestructive Evaluation*, vol. 38, no. 1, pp. 1-7, 2019.
- [14] Y. Q. Peng and H. H. Huang, "Mechanical and magnetic properties of TRIP690 steel strengthened by strain-induced martensite," *Journal of Magnetism and Magnetic Materials*, vol. 550, pp. 169083, 2022.
- [15] G. Vertesy, I. Meszaros, and I. Tomas, "Nondestructive magnetic characterization of TRIP steels," *NDT & E International*, vol. 54, pp. 107-114, 2023.
- [16] NML Technology Handbook, "National Metallurgical Laboratory (NML)," *NML Technology Handbook*, 2019. [Online]. Available: <https://transparency.nmlindia.org/ta/NML-Technology-Handbook.pdf>. [Accessed: May 29, 2021].
- [17] X. F. Chen, J. W. Liang, D. P. Yang, Z. P. Hu, X. Xu, X. L. Gu, and G. M. Xie, "Effect of chromium on microstructure and mechanical properties of hot-dip galvanized Dual-Phase (DP980) steel," *Crystals*, vol. 13, no. 8, pp. 1287, 2023.
- [18] M. Soleimani, A. Kalhor, and H. Mirzadeh, "Transformation-Induced Plasticity (TRIP) in advanced steels: A review," *Materials Science and Engineering: A*, vol. 795, pp. 140023, 2020.